Bioconjugate Chemistry

Article

pubs.acs.org/bc

# Assembling Multiporphyrin Stacks Inside the DNA Double Helix

Mykhailo Vybornyi,[†] Alina L. Nussbaumer, Simon M. Langenegger,[†] and Robert Häner*[,†]

[†]Department of Chemistry and Biochemistry, University of Bern, Freiestrasse 3, CH-3012 Bern, Switzerland

Supporting Information

**ABSTRACT:** Double stranded DNA hybrids containing up to four consecutive, face-to-face stacked porphyrins are described. Non-nucleosidic, 5,15-bisphenyl-substituted porphyrin building blocks were incorporated into complementary oligonucleotide strands. Upon hybridization multiple porphyrins are well accommodated inside the DNA scaffold without disturbing the overall B-DNA structure. The formation of double strands containing up to four free base porphyrins is enabled without compromising duplex stability. UV/vis, fluorescence, and CD spectroscopy demonstrate the formation of porphyrins H-aggregates inside the DNA double helix and provide evidence for the existence of strong excitonic coupling between interstrand stacked porphyrins. H-aggregation results in considerable fluorescence quenching. Most intense CD effects are observed in stacks containing four porphyrins. The findings demonstrate the value of DNA for the controlled formation of molecularly defined porphyrin aggregates.

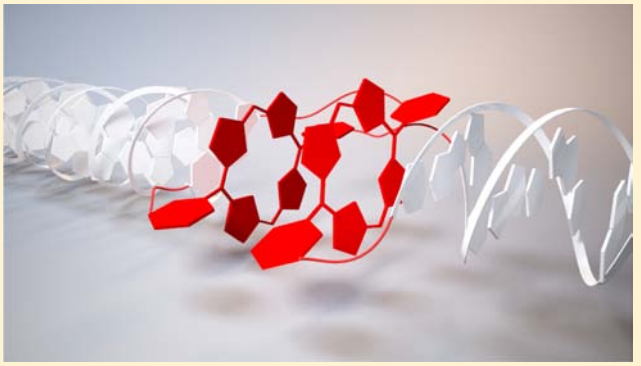

## INTRODUCTION

The development of supramolecular architectures for the controlled preparation of porphyrin arrays has received considerable attention over the last decades.[1−4] The interest originates largely from the desire to mimic naturally occurring light-harvesting complexes, in which efficient energy transfer is enabled by the interaction of highly ordered, protein-bound porphyrins.[5−9] Modern materials science intends to elaborate suitable approaches toward artificial systems with tunable optoelectronic properties.[10−12] Chromophore organization can be elegantly achieved by the site-specific functionalization of DNA.[13−21] The use of modified phosphoramidites allows placing functional molecules in a DNA network with high precision.[22−24] Modifications of DNA are routinely achieved by chemical alteration of the nucleobases or the sugar, as well as through linkages to the phosphate backbone.[25−28] The integration of porphyrin into DNA by the solid-phase method for structural investigations was pioneered by Richert.[29] Since then, the number of applications of porphyrin−DNA conjugates has continuously grown.[30−36] Balaz and Berova introduced porphyrin end-caps[37,38] as effective optical reporters for structure-sensitive studies of DNA.[39−41] The construction of porphyrin arrays along DNA of up to 11 molecules was reported by Stulz.[42] Among the large number of papers on porphyrin−DNA conjugates,[43−56] few reports describe the use of non-nucleosidic derivatives as base pair surrogates.[29,50,57,58] Recently, Zhang investigated the interactions of porphyrins in GNA in detail[58] and the authors clearly established face-to-face stacking of two porphyrin molecules in the double helix. Yet, questions about the structural and electronic interactions of larger arrays of porphyrins stacked inside a double-stranded DNA remained. Additional studies on multiporphyrin systems are essential for the general understanding of chromophore interactions and may help in the design and construction of discrete molecular wires.

This study describes the preparation and the properties of porphyrin segments of up to four units within a DNA duplex. We demonstrate that porphyrins preferably form H-aggregates in a double helical framework. The close spatial proximity of the chromophores leads to excitonic interactions which are evident from UV/vis, fluorescence, and CD data. Furthermore, the thermal denaturation experiments display that $\pi$-stacking interactions of porphyrins contribute significantly to duplex stability.

## RESULTS AND DISCUSSION

**Synthesis of the Porphyrin Phosphoramidite and Preparation of Oligonucleotides.** The required phosphoramidite building block suitable for solid-phase DNA synthesis was prepared as shown in Scheme 1. Condensation of aldehyde **1**, prepared from 3-bromobenzaldehyde and 4-pentyn-1-ol, with 2,2′-dipyrromethane (**2**)[59] in the presence of trifluoroacetic acid gave the bis-hydroxy derived porphyrin **3**. Compound **3** shows the typical spectroscopic features of porphyrins. The UV-spectrum of **3** in organic solvents, such as THF, exhibits an intense Soret band at 412 nm and four low-intensity Q-bands (see Supporting Information (SI), Figure S1). Subsequent protection of **3** with 4,4′-dimethoxytrityl chloride provided derivative **4**, which was converted into phosphoramidite **5**. The average stepwise coupling yields

**Received:** July 7, 2014
**Revised:** August 7, 2014
**Published:** September 3, 2014

   dx.doi.org/10.1021/bc500297e | *Bioconjugate Chem.* 2014, 25, 1785−1793

**Scheme 1. Synthesis of Phosphoramidite 5**

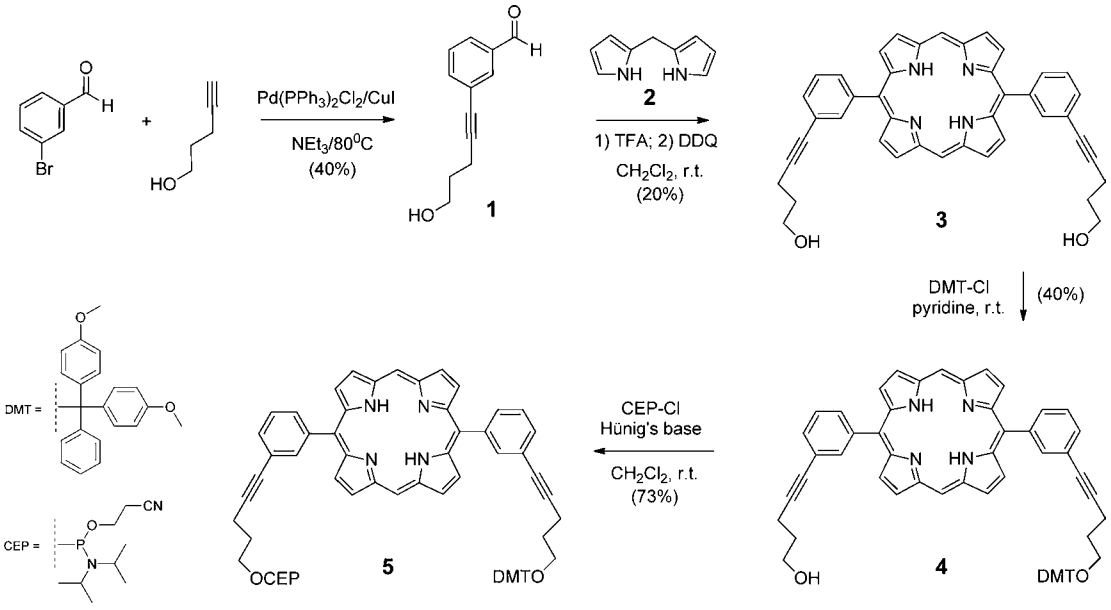


**Scheme 2. DNA Sequences Used in This Study and Schematic Illustration of Different Types of Hybrids Investigated**[a]

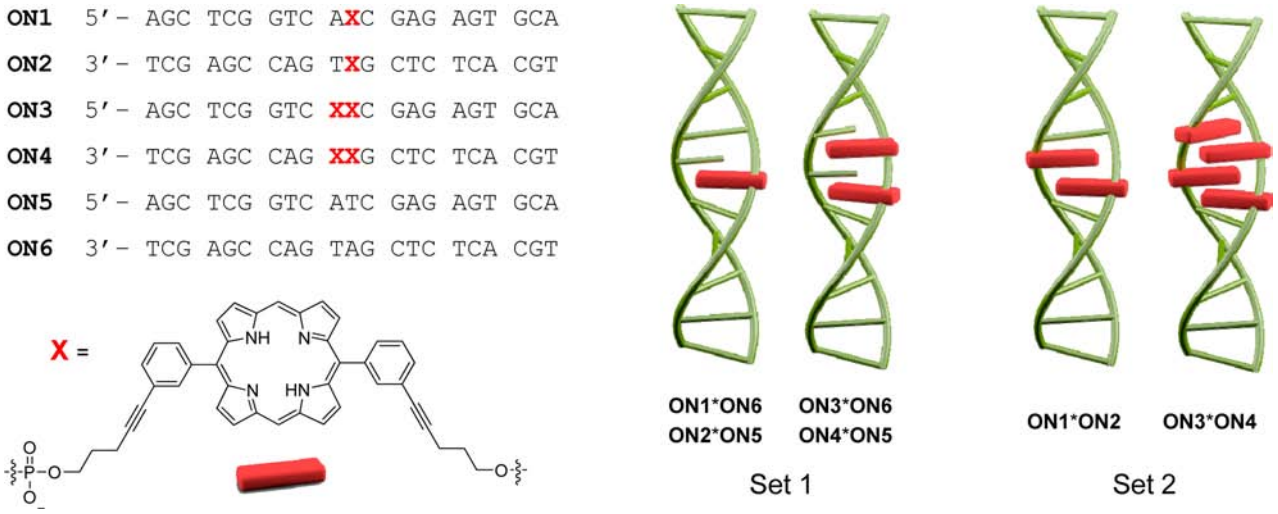


[a]Set 1 includes hybrids containing porphyrins opposite a natural nucleobase; hybrids in Set 2 have one or two porphyrin modifications in each strand positioned as shown.

obtained for incorporation of **5** during automated oligonucleotide synthesis were approximately 80% using a coupling time of 600 s. Four oligonucleotides (**ON1**−**ON4**, Scheme 2) containing one or two porphyrin units were synthesized and purified by RP HPLC and their molecular weights were confirmed by MS (see Experimental Section and SI). **ON5** and **ON6** serve as reference oligonucleotides.

**Hybrid Stability.** Thermal denaturation experiments were carried out to establish the influence of the porphyrin modification on duplex stability. Melting curves were measured in the nucleobase region (260 nm) and at the Soret band (SI Figures S3−S5). The melting temperatures ($T_m$) are summarized in Table 1. Hybrid **ON5***ON6**, which is used as the unmodified reference duplex, has a $T_m$ of 72 °C. All hybrids carrying porphyrin molecules opposite a natural base (Set 1, see Scheme 2) show a relatively large decrease in the $T_m$ ($\Delta T_m$ ~10−16 °C). This observation is in agreement with previous findings that incorporation of one[29,50,57] or several[42] porphyrins in the absence of interstrand porphyrin−porphyrin interactions leads to a considerable reduction of duplex stability. Obviously, stacking and hydrophobic interactions between porphyrin and the DNA cannot counterbalance the energetic cost associated with the loss of an AT base pair. On the other hand, hybrids of Set 2 containing one or two modifications in opposite positions possess approximately the same thermal stabilities as the unmodified duplex. Thus, porphyrin−porphyrin interstrand interactions compensate for the loss of binding energy of a canonical base pair.

**UV/vis Spectroscopy.** Porphyrin interactions are conveniently monitored by UV/vis spectroscopy. The most prominent changes occur in the Soret region. Absorption spectra of single strands **ON1**−**ON4** are shown in Figure 1. All oligomers exhibit the signals expected for porphyrin−DNA conjugates: the Soret band around 400 nm and four Q-bands (~500−640


dx.doi.org/10.1021/bc500297e | Bioconjugate Chem. 2014, 25, 1785−1793

Table 1. Spectroscopic and $T_m$ Data of Porphyrin-Modified Single and Double Strands[a]

| Sequence | $\lambda_{max}$/nm 20 °C | log $\varepsilon$ 20 °C | $\lambda_{max}$/nm 90 °C | $\Delta\lambda$/nm[b] | Q-bands $\lambda_{max}$/nm 20 °C | $T_m$ ($\Delta T_m$)[c] | $\lambda_{em}$/nm 20 °C | $\lambda_{em}$/nm 90 °C | $\Phi_f$[i] 20 °C | H[j], % |
|---|---|---|---|---|---|---|---|---|---|---|
| **ON1** | 411 | 5.55 | 408 | 3 | 508, 542, 576, 632 | n/d | 634; 696[g] | 635; 697[g] | 0.96[g] | 6 |
| **ON2** | 414 | 5.52 | 408 | 6 | 508, 544, 579, 633 | n/d | 636; 700[g] | 635; 697[g] | 1.00[g] | 9 |
| **ON3** | 392 | 5.07 | 391 | 1 | 510, 547, 580, 636 | n/d | 641; 706[h] | 642; 705[h] | 0.20[h] | 60 |
| **ON4** | 395 | 5.27 | 391 | 4 | 510, 547, 580, 636 | n/d | 641; 706[h] | 642; 705[h] | 0.16[h] | 14 |
| | | | | | Set 1 | | | | | |
| **ON1*ON6** | 410 | 5.54 | 408 | 2 | 507, 541, 575, 632 | 61.4 °C[d] (−10.6) | 633; 695[g] | 636; 698[g] | 0.96[g] | 8 |
| **ON2*ON5** | 408 | 5.54 | 408 | 0 | 507, 541, 573, 626 | 60.2 °C[d] (−11.8) | 631; 694[g] | 636; 698[g] | 0.90[g] | −3 |
| **ON3*ON6** | 392 | 5.26 | 391 | 1 | 511, 547, 580, 635 | 62.8 °C[d] (−9.2) | 642; 705[h] | 642; 706[h] | 0.23[h] | 3 |
| **ON4*ON5** | 394 | 5.35 | 391 | 3 | 511, 546, 579, 634 | 56.0 °C[d] (−16.0) | 642; 705[h] | 642; 706[h] | 0.19[h] | 11 |
| | | | | | Set 2 | | | | | |
| **ON1*ON2** | 391 | 5.32 | 408 | −17 | 510, 547, 577, 633 | 72.2 °C[d,e] (+0.2) | 638; 699[g] | 635; 697[g] | 0.73[g]; 0.33[h] | 76 |
| **ON3*ON4** | 390 | 4.97 | 391 | −1 | 510, 545, 580, 635 | 70.0 °C[d,f] (−2.0) | 643; 708[h] | 642; 705[h] | 0.14[g]; 0.18[h] | 102 |

[a]Conditions: 1 $\mu$M of each strand, 10 mM sodium phosphate buffer pH = 7.2, 100 mM NaCl, 1 mM $Na_2EDTA$. [b]$\lambda_{max}$(20 °C) − $\lambda_{max}$(90 °C) of the Soret bands. [c]Relative to the unmodified duplex **ON5*ON6** ($T_m$ = 72.0 °C), estimated error ±1 °C. [d]Value determined at 260 nm. [e]Value determined at 408 nm. [f]Value determined at 391 nm. [g]$\lambda_{ex}$: 408 nm. [h]$\lambda_{ex}$: 391 nm. [i]Quantum yield relative to the oligomer **ON2**, which was defined as 1.0 (for details see SI). [j]Hyperchromicity, the value was calculated from the Soret band maxima at 20 and 90 °C.

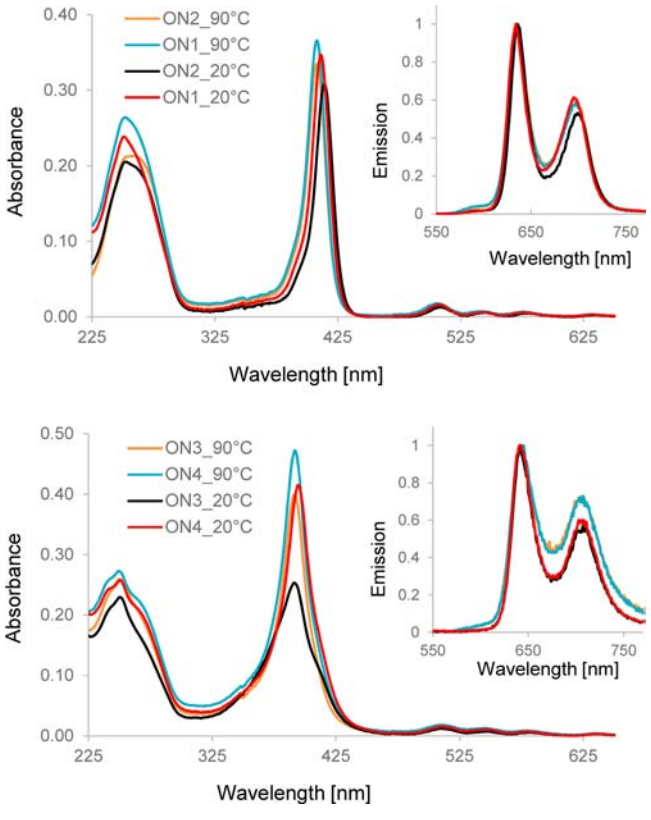


**Figure 1.** Absorption and normalized emission (inset) spectra of single strands containing one (top) or two (bottom) porphyrin units. Conditions: see Table 1; $\lambda_{ex}$ 408 nm (**ON1**, **ON2**) and 391 nm (**ON3**, **ON4**).

nm); the region below 300 nm is dominated by the absorption of the nucleobases. All numerical data are summarized in Table 1. The hydrophobic aromatic part of DNA also supports stacking interactions in single strands. In the present case, interactions between nucleobases and porphyrins as well as between two adjacent porphyrins (possible in **ON3** and **ON4**) are confirmed by changes in the position of the Soret band.[60] A blue-shift of 19 nm is observed between the oligomers containing a single (**ON1**, **ON2**) and those containing two adjacent porphyrin modification (**ON3**, **ON4**, Table 1, $\lambda_{max}$@ 20 °C). A blue-shift of this magnitude suggests the presence of face-to-face interactions of the neighboring porphyrins. In single strands with one modification, the interaction between porphyrin and nucleobases can be followed in temperature-dependent experiments. Thus, a red-shift is observed in **ON1** (3 nm) and **ON2** (6 nm) when the temperature is decreased from 90 to 20 °C (Table 1, column $\Delta\lambda$). Hypochromicities measured at the Soret band are small (<10%) in oligomers containing a single porphyrin unit (**ON1** and **ON2**) and larger in those with two consecutive moieties (**ON3** and **ON4**; 60% and 14%).

Absorption spectra of the different double stranded hybrids are given in Figure 2. Set 1 comprises the strand combinations in which only *intrastrand* porphyrin interactions are possible. The UV/vis spectra of these oligomers in dissociated (90 °C) and hybridized form (20 °C) are depicted in Figure 2. Duplex formation is accompanied by minor changes in the porphyrin absorbance region. For example, the Soret band is not (**ON2*ON5**) or only slightly red-shifted upon cooling, i.e., hybrid formation (see Table 1, $\Delta\lambda$). Also, the hyperchromicity for the maximum of the porphyrin absorbance is rather small for these samples (≤11%).

Spectroscopic effects are much more significant in Set 2. This set contains the strands which, upon duplex formation, bring together porphyrins from the two single strands, thus assembling porphyrin stacks inside the DNA double helix. Formation of interstrand stacks results in strong excitonic interactions between porphyrins. Hybridization of **ON1** and **ON2**, which bring together two porphyrins (Figure 3, top), results in a considerable blue shift of the Soret band (391 nm in the hybrid vs 411 and 414 nm in the single strands). A second, weaker signal (shoulder) appears at 408 nm. Thermal denaturation at 90 °C leads to the complete disappearance of the 391 nm band and concurrent growth of the 408 nm band (see Figure 4). At the same time, a strong hyperchromicity


dx.doi.org/10.1021/bc500297e | Bioconjugate Chem. 2014, 25, 1785−1793

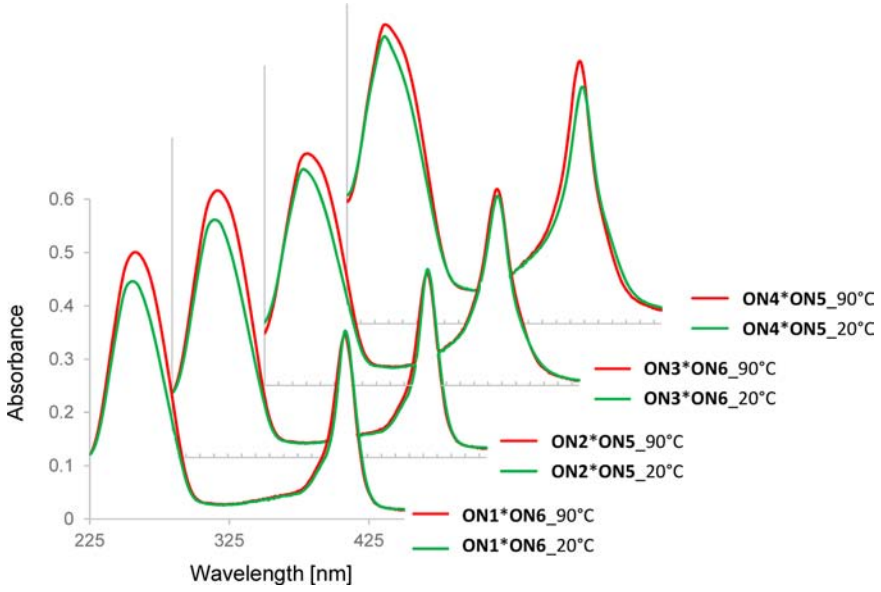


**Figure 2.** Temperature effect (90 vs 20 °C) in UV/vis spectra observed for oligomer combinations of Set 1. Conditions: see Table 1.

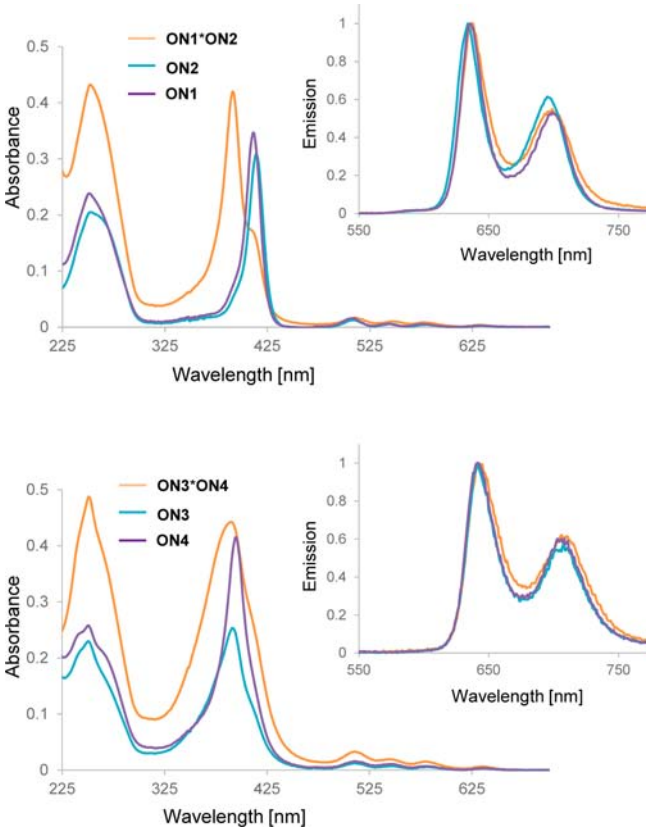


**Figure 3.** Absorption and normalized emission (inset) spectra of hybrids and single strands of Set 2 at 20 °C. Conditions: see Table 1; $\lambda_{ex}$ = 408 nm (**ON1**, **ON2**) and 391 nm (**ON3**, **ON4**).

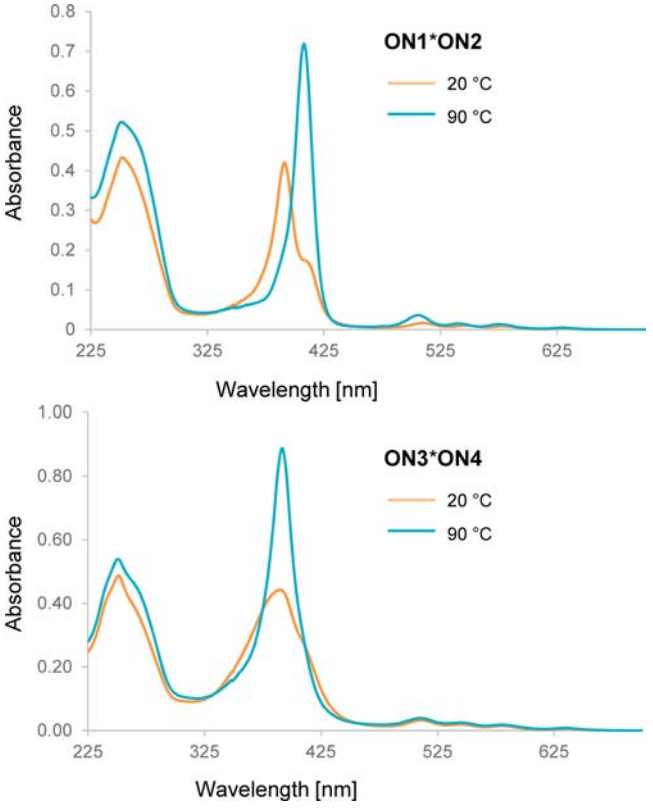


**Figure 4.** Temperature effect (90 vs 20 °C) in UV/vis spectra observed for oligomer combinations of Set 2. Conditions: see Table 1.

(76%, Table 1) is observed. These changes provide strong support for the presence of H-type interaction.[61−63] Along with the blue shift of the Soret band, formation of porphyrin H-aggregates has been reported to result in a red shift of the Q-bands.[64] Such a red shift, albeit to a slight extent, is also observed in the present system (see, e.g., Table 1). The formation of the hybrid **ON3***ON4**, which results in a stack of four porphyrins, is accompanied by a more complex behavior. A substantial broadening of the Soret band (maximum at 390 nm) occurs, suggesting the presence of multiple electronic interactions between the individual porphyrin molecules (Figure 3, bottom). Additionally, a strong hyperchromicity of ∼100% results from thermal dissociation. In summary, UV/vis data support a model in which the hydrophobic porphyrins are assembled in between the DNA base stack, thus maximizing $\pi$-


dx.doi.org/10.1021/bc500297e | *Bioconjugate Chem.* 2014, 25, 1785−1793

stacking interactions and minimizing exposure to the aqueous environment.

**Fluorescence Spectroscopy.** The emission spectra of porphyrin-modified single strands exhibit the characteristic pattern of free-base porphyrin fluorescence. Upon excitation at the Soret band, two separate emission bands are observed for all samples in the area of 600−750 nm (Figure 1, insets). The normalized emission spectra of **ON1** and **ON2** or **ON3** and **ON4** are essentially superimposable. Emission maxima of **ON3** and **ON4** are red-shifted (5−10 nm) compared to **ON1** and **ON2** (Table 1, column $\lambda_{em}$). When two porphyrins are adjacent, their stacking leads to a quenching of the fluorescence. Thus, single strands **ON1** and **ON2** have higher quantum yields ($\Phi_f$, Table 1) relative to **ON3** and **ON4**, which is in agreement with the general observation that fluorescence of porphyrin H-aggregates is quenched. Emission spectra of the double strands of Set 1 are similar to those of the single strands. This includes a small red shift of the emission bands of hybrids **ON3*ON6** and **ON4*ON5** compared to the duplexes containing a single porphyrin incorporation. Furthermore, the relative quantum yields are hardly changed upon duplex assembly.

In Set 2, duplex formation does not result in substantial changes in the shape of the fluorescence spectra with respect to the single strands (Figure 3, insets). However, the relative quantum yield ($\Phi_f$, Table 1) strongly depends on the excitation wavelength in hybrid **ON1*ON2**. It equals 0.73 when excited at 408 nm compared to 0.33 after excitation at 391 nm. This difference can again be rationalized by fluorescence quenching due to H-aggregation (391 nm). In hybrid **ON3*ON4**, however, the excitation wavelength exhibits a modest influence on $\Phi_f$, which is 0.18 (408 nm) and 0.14 (391 nm). Interestingly, combining four porphyrin units by annealing **ON3** and **ON4** within a DNA scaffold doubles the size of the stack without a substantial loss in the quantum yield.

**Excitation Spectra.** For the single strands **ON1** and **ON2** containing a single porphyrin unit, absorption and excitation spectra in the region of the Soret band coincide entirely (SI, Figure S7). For doubly modified single strands (**ON3** and **ON4**) a modest broadening is observed due to electronic interaction of the neighboring porphyrin rings. Hybrids of Set 1 show very similar behavior as the single strands (SI, Figure S8). The picture changes with hybrids of Set 2, in particular, for **ON1*ON2** (Figure 5, top). Absorption and excitation spectra for this hybrid differ significantly in the 370−420 nm region. As described above (Figures 3 and 4), interstrand stacking of the porphyrins leads to the splitting of the Soret band in the absorption spectrum into a high-intensity blue-shifted and a low-intensity red-shifted component. In the excitation spectrum, however, the signal intensity is reversed with the 408 nm band being dominant. This is in alignment with the general observation that the formation of H-aggregates (blue-shifted band) results in a reduction of emission intensity.[65] These features are less well recognized in hybrid **ON3*ON4** (Figure 5, bottom) since signals are considerably broadened due to aggregation of four porphyrins.

**CD Spectroscopy.** Porphyrins are well-documented reporters for structural studies on the basis of excitonic coupling.[66,67] Single strands **ON1** and **ON2** exhibit weak or no CD effects in the region of the Soret band (see SI Figure S9). A weak induced CD signal at 408 nm is observed ($\Delta\varepsilon$ = 20 $M^{-1}$ $cm^{-1}$) for **ON1**. Similar findings were reported for a different type of single-stranded porphyrin−DNA conjugates.[68]

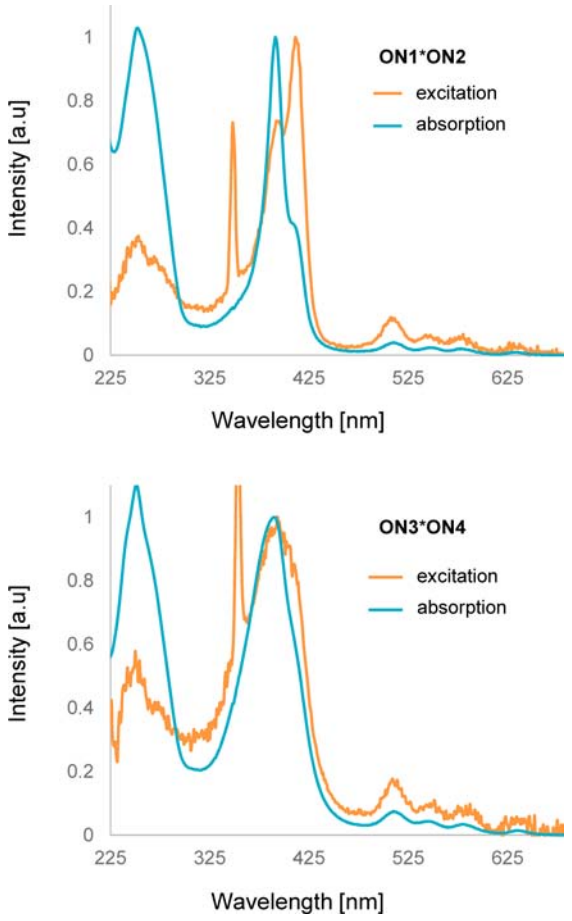


**Figure 5.** Normalized UV/vis absorption and excitation spectra at 20 °C. Conditions: see Table 1; $\lambda_{ex}$ 696 nm (**ON1*ON2**) and 706 nm (**ON3*ON4**).

No significant signals are present for **ON2** in the 400 nm region. For **ON3**, which has two adjacent porphyrins, a strong, complex signal (430 nm, $\Delta\varepsilon$ = +15 $M^{-1}$ $cm^{-1}$ and 387 nm, $\Delta\varepsilon$ = −54 $M^{-1}$ $cm^{-1}$) is observed. **ON4** exhibits only a very weak positive signal 391 nm. All aforementioned features disappear after unfolding of the strands at 90 °C (SI Figure S9).

CD spectra of duplexes are displayed in Figure 6. All hybrids exhibit the typical DNA B-form signal in the nucleobase absorbance region. Thus, porphyrins are well accommodated in the double helix without perturbing the B-DNA structure to a significant extent. For example, both **ON1*ON6** and **ON2*ON5** have a weak induced CD ($\Delta\varepsilon$ = −13 $M^{-1}$ $cm^{-1}$ and −10 $M^{-1}$ $cm^{-1}$, respectively) with a maximum almost coinciding with the Soret band (see also SI Figure S10). This type of CD signal is strongly reminiscent of DNA-intercalated cationic porphyrins.[69−71] CD spectra of **ON3*ON6** show a bisignate profile (424 nm, $\Delta\varepsilon$ = +8 $M^{-1}$ $cm^{-1}$ and 394 nm, $\Delta\varepsilon$ = −15 $M^{-1}$ $cm^{-1}$), whereas hybrid **ON4*ON5** is basically CD silent in this region. The most significant effects are observed in Set 2. Interstrand porphyrin interactions in duplex **ON1*ON2** lead to a bisignate Cotton effect due to exciton coupling (438 nm, $\Delta\varepsilon$ = −23 $M^{-1}$ $cm^{-1}$ and 418 nm, $\Delta\varepsilon$ = +17 $M^{-1}$ $cm^{-1}$). Interestingly, the center of the couplet lies in the region of the red-shifted absorption shoulder (see SI Figure S11). Negligible CD activity is present, however, at the dominant absorption signal (391 nm, Figure 3) ascribed to H-type (face-to-face) aggregation. Finally, aggregation of four porphyrins in duplex


dx.doi.org/10.1021/bc500297e | Bioconjugate Chem. 2014, 25, 1785−1793

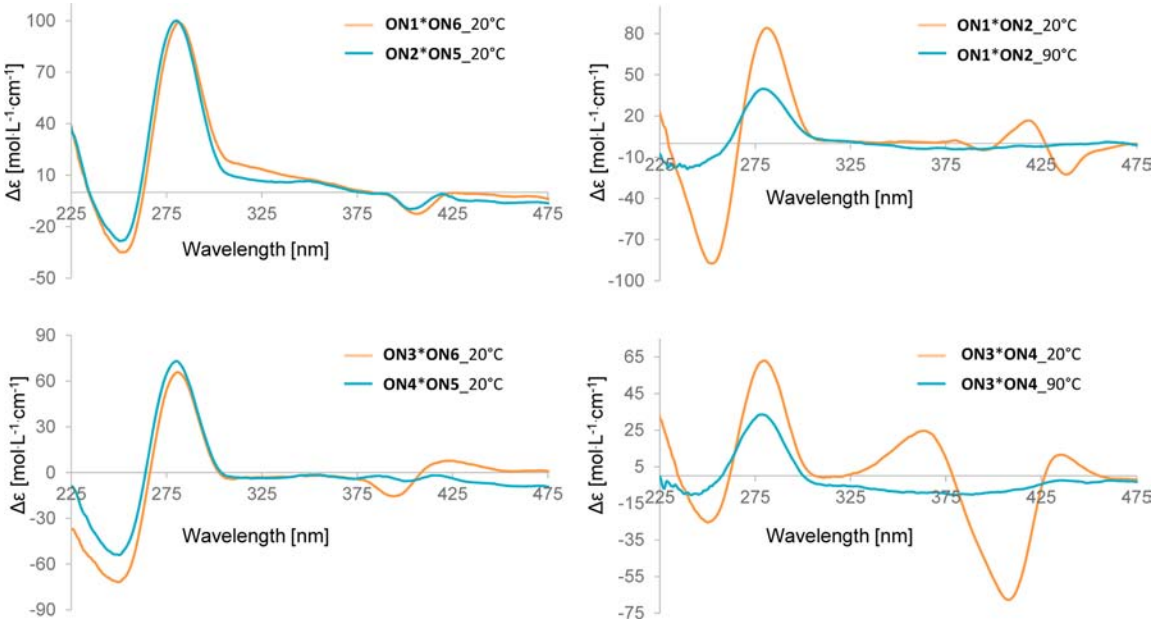


**Figure 6.** CD spectra of double strands (left: Set 1; right: Set 2 at different temperature). Conditions: see Table 1.

**ON3*ON4** gives rise to very intense signals. At the same time, these signals are also rather complex (435 nm, $\Delta\varepsilon$ = +12 $M^{-1}$ $cm^{-1}$, 408 nm, $\Delta\varepsilon$ = −68 $M^{-1}$ $cm^{-1}$ and 364 nm, $\Delta\varepsilon$ = +25 $M^{-1}$ $cm^{-1}$), which can be ascribed to the presence of multiple porphyrin interactions.[72] Again, all features disappear upon heating to 90 °C, showing that the structural organization of the porphyrins is governed by the DNA supramolecular framework. The present approach demonstrates that multiple porphyrins can be arranged in an intrahelical manner. A face-to-face stacking arrangement is manifested by pronounced exciton coupling and H-aggregation. This design enables the assembly of well-defined porphyrin stacks and, at the same time, the intrahelical organization reduces the potential for interhelical aggregation.[51]

## SUMMARY AND CONCLUSIONS

In summary, we have presented the synthesis and spectroscopic characterization of porphyrin−DNA conjugates. The required phosphoramidite building block is accessible by a short, four-step synthesis from commercially available reagents. Modified oligonucleotides are prepared by incorporation of one or two non-nucleosidic, 5,15-bisphenyl-substituted porphyrins via phosphoramidite chemistry. Hybridization of complementary strands enables the formation of duplexes containing up to four consecutive free base porphyrins. Pairwise placement of porphyrins in opposite positions maintains duplex stability, whereas a considerable reduction in the $T_m$ is observed when porphyrins are positioned opposite to natural nucleobases ($\Delta T_m$ up to −12 °C per modification). UV/vis spectroscopy supports a model of H-aggregated porphyrins assembled inside the DNA double helix. H-aggregation results in considerable fluorescence quenching. Furthermore, CD spectroscopy provides additional evidence for substantial excitonic coupling of interstrand stacked porphyrins; in particular, strong CD effects are observed in the duplex with four stacked porphyrins. Notably, stacks of multiple porphyrins are well accommodated inside the DNA scaffold without disturbing the overall B-DNA structure and duplex stability. The present findings demonstrate the value of DNA for the controlled formation of molecularly defined porphyrin aggregates.

## EXPERIMENTAL PROCEDURES

The synthetic route leading to the phosphoramidite building block and the porphyrin-modified oligodeoxynucleotides is shown in Schemes 1 and 2, respectively.

**3-(5-Hydroxypent-1-ynyl)benzaldehyde (1).** 4-Bromobenzaldehyde (3 mL, 26 mmol), $Pd(PPh_3)_2Cl_2$ (105 mg, 0.15 mmol), and CuI (55 mg, 1.5 mmol) were placed in a reaction flask. After heating to 80 °C, triethylamine (50 mL) and 4-pentyn-1-ol (3 mL, 31 mmol) were added. The reaction mixture was stirred at 80 °C overnight. After cooling to room temperature, 20 mL of EtOAc were added and a gray precipitate was removed by filtration, and the filtrate was concentrated. The product was purified by column chromatography ($SiO_2$, EtOAc/hexane, 1:2), which furnished 1.9 g (yield 40%) of **1**. Analytical data for **1**: $R_f$ = 0.36 ($SiO_2$, EtOAc/hexane, 1:2). $^1$H NMR (300 MHz, DMSO), $\delta$: 9.99 (s, 1H, −C*H*O), 7.92−7.81 (m, 2H, −C$H_{ar}$), 7.70 (d, $J$ = 7.7 Hz, 1H, −C$H_{ar}$), 7.58 (t, $J$ = 7.6 Hz, 1H, −C$H_{ar}$), 4.56 (t, $J$ = 5.1 Hz, 1H, −O*H*), 3.54 (dd, $J$ = 11.5, 6.0 Hz, 2H, −C$H_2$OH), 2.50 (t, $J$ = 7.1 Hz, 2H, −C$H_2$C$H_2$C$H_2$), 1.71 (t, $J$ = 6.6 Hz, 2H, −C$H_2$C$H_2$OH). $^{13}$C NMR (75 MHz, DMSO), $\delta$: 192.6, 136.7, 136.4, 132.4, 129.5, 128.2, 124.2, 92.2, 79.2, 59.4, 31.4, 15.3. HRMS for $C_{12}H_{12}O_2$: found 188.0834 (calculated 188.0821).

**5,15-Bis-3-(5-hydroxypent-1-ynyl)phenylporphyrin (3).** Compounds **1** (500 mg, 3.42 mmol) and **2**[59] (640 mg, 3.42 mmol) were dissolved in dry $CH_2Cl_2$ (300 mL). TFA (0.45 mL) was added dropwise. The reaction mixture was stirred at room temperature for 2 h, and DDQ (770 mg, 3.42 mmol) was added. The dark brown solution was stirred overnight. Afterward, the reaction mixture was filtered through AlOx using $CH_2Cl_2$/MeOH 96/4 system as eluent. The filtrate was concentrated and purified by flash chromatography on AlOx. The solvents were evaporated and the precipitate was collected. This furnished 228 mg (yield 20%) of the title compound **3**. Analytical data for **3**: $R_f$ = 0.3 (AlOx, $CH_2Cl_2$/MeOH 96/4). $^1$H NMR (300 MHz, DMSO), $\delta$: 10.66 (s, 2H, meso−C*H*),


dx.doi.org/10.1021/bc500297e | Bioconjugate Chem. 2014, 25, 1785−1793

9.68 (d, $J$ = 4.7 Hz, 4H, −C*H* from a porphyrin core), 9.02 (d, $J$ = 4.6 Hz, 4H, −C*H* from a porphyrin core), 8.24 (d, $J$ = 2.2 Hz, 4H, −C$H_{ar}$), 8.03−7.72 (m, 4H, −C$H_{ar}$), 3.54 (t, $J$ = 6.2 Hz, 4H, −C$H_2$OH), 2.58−2.50 (t, 4H, −C$H_2$C$H_2$C$H_2$), 1.73 (t, $J$ = 6.6 Hz, 4H, −C$H_2$C$H_2$OH), −3.33 (s, 2H, −N*H*). The $^{13}$C NMR was difficult to measure due to a low solubility of **3**. HRMS (M+H$^+$) for $C_{42}H_{35}N_4O_2^+$: found 627.2740 (calculated 627.2755).

**15-3-[(5-Hydroxypent-1-ynyl)phenyl]-5-3-{[bis(4-methoxyphenyl)phenylmethoxy]-(pent-1-ynyl)phenyl}-porphyrin (4).** A solid 4,4′-dimethoxytrityl chloride (115 mg, 0.34 mmol) was added dropwise to solution of **3** (228 mg, 0.34 mmol) in dry pyridine (10 mL). The mixture was stirred overnight, and the solvent was evaporated. The residue was dissolved in a small volume of $CH_2Cl_2$ and subjected to column chromatography (AlOx, $CH_2Cl_2$/MeOH/$NEt_3$ 97.5/2/0.5). This furnished 125 mg (yield 38%) of purple crystals. Analytical data for **4**: $R_f$ = 0.45 (AlOx, $CH_2Cl_2$/MeOH/$NEt_3$ 97.5/2/0.5); $^1$H NMR (300 MHz, DMSO), $\delta$: 10.66 (s, 2H, meso−C*H*), 9.67 (s, 4H, −C*H* from a porphyrin core), 9.01 (dd, $J$ = 8.8, 4.6 Hz, 4H, −C*H* from a porphyrin core), 8.25 (s, 3H, −C$H_{ar}$), 8.10 (s, 1H, −C$H_{ar}$), 7.9−7.71 (m, 4H, −C$H_{ar}$), 7.45−7.04 (m, 8H, −C$H_{ar}$), 6.88−6.78 (t, $J$ = 25.4 Hz, 5H, −C$H_{ar}$), 4.53 (s, 1H, −O*H*), 3.54 (d, $J$ = 5.5 Hz, 2H, −C$H_2$OH), 3.43 (s, 6H, −O$CH_3$), 3.14 (s, 2H, −C$H_2$ODMT), 2.59 (d, $J$ = 26.9 Hz, 4H, −C$H_2$C$H_2$C$H_2$), 1.76 (dd, $J$ = 23.7, 17.0 Hz, 4H, −C$H_2$C$H_2$OH), −3.31 (s, 2H, −N*H*). $^{13}$C NMR (75 MHz, DMSO), $\delta$: 157.8, 146.2, 144.9, 140.7, 136.8, 135.9, 133.9, 132.7, 130.7, 129.5, 127.6, 126.8, 126.3, 122.2, 117.6, 112.9, 105.8, 90.9, 85.2, 80.6, 61.3, 59.4, 54.6, 31.5, 28.4, 15.6. HRMS for $C_{63}H_{52}N_4O_2$: found 928.3981 (calculated 928.2983).

**15-3-[(5-Hydroxypent-1-ynyl)phenyl]-5-3-{[bis(4-methoxyphenyl)phenylmethoxy]-(pent-1-ynyl)phenyl}-porphyrin cyanoethyl (diisopropylamino)-phosphoramidite (5).** Compound **4** (125 mg, 0.128 mmol) was dissolved in $CH_2Cl_2$ (10 mL). After addition of DIPEA (150 μL), a solution of 2-cyanoethyl-*N*,*N*-diisopropylchlorophosphoramidite (40 mg, 0.166 mmol, 1.3 equiv) was added. The mixture was stirred for 3 h. The solvent was evaporated, and the residue was dissolved in EtOAc/$NEt_3$ 99.5/0.5 and purified by column chromatography (EtOAc/$NEt_3$ 99.5/0.5), furnished 110 mg (yield 73%) of **5** as a dark brown foam. Analytical data for **5**: $R_f$ = 0.9 (AlOx, EtOAc/$NEt_3$ 99.5/0.5); $^1$H NMR (300 MHz, DMSO), $\delta$: 10.65 (s, 2H, meso−C*H*), 9.65 (dd, $J$ = 4.6, 1.9 Hz, 4H, −C*H* from a porphyrin core), 9.00 (dd, $J$ = 7.0, 4.7 Hz, 4H, −C*H* from a porphyrin core), 8.24 (s, 3H, −C$H_{ar}$), 8.10 (d, $J$ = 4.1 Hz, 1H, −C$H_{ar}$), 7.94−7.70 (m, 4H, −C$H_{ar}$), 7.48−7.00 (m, 8H, −C$H_{ar}$), 6.90−6.71 (dd, $J$ = 51.7, 7.1 Hz, 5H, −C$H_{ar}$), 3.81−3.63 (m, 4H, −C$H_2$ aliphatic), 3.57−3.47 (m, 2H, −C$H_2$ aliphatic), 3.42 (s, 6H, −O$CH_3$), 3.14 (t, $J$ = 6.0 Hz, 2H, −C$H_2$ODMT), 2.77−2.55 (m, 6H, 4 × −C$H_2$C$H_2$C$H_2$ and 2 × −C*H*C$H_3$), 1.85 (s, 4H, −C$H_2$C$H_2$OH), 1.10−0.98 (m, 12H, −CHC$H_3$), −3.31 (s, 2H, −N*H*). $^{13}$C NMR (75 MHz, DMSO), $\delta$: 157.8, 146.2, 144.9, 140.7, 140.7, 136.8, 136.8, 135.9, 134.0, 132.7, 130.7, 130.6, 129.5, 127.6, 126.3, 122.2, 118.8, 117.6, 112.9, 105.9, 90.6, 85.2, 80.8, 61.5, 58.1, 54.6, 42.34, 29.1, 24.3, 19.8, 15.6. $^{31}$P NMR (122 MHz, DMSO), $\delta$: 146.64. HRMS (M+H$^+$) for $C_{72}H_{70}N_6O_5P^+$: found 1129.5136 (calculated 1129.5140).

**Oligonucleotide Synthesis and Purification.** Oligonucleotides were prepared via automated DNA synthesis by a standard synthetic procedure ("trityl-off" mode) on a 394-DNA/RNA synthesizer (Applied Biosystems Instruments). The coupling time for phosphoramidite **5** (0.1 M solution in THF) was elongated to 600 s. Cleavage from the solid support and final deprotection were performed without delay after completion of the oligonucleotide synthesis by treatment with 27% aqueous ammonia solution (Aldrich, Trace Select; note: the use of high quality ammonia considerably reduces metal contamination) at 55 °C for 16 h. All oligonucleotides were purified by reverse-phase HPLC (LiChrospher 100 RP-8, 5 μm, Merck, Bio-Tek Instruments); eluent A = ($Et_3$NH)OAc (0.01 M, pH 7.0)/$CH_3CN$ in 80/20 v/v; eluent B = $CH_3CN$; gradient 0−40% B over 22 min, then 40−100% B over 5 min. Mass spectrometry of oligonucleotides was carried out with a Sciex QSTAR pulsar (hybrid quadrupole time-of-flight mass spectrometer, Applied Biosystems).

## ■ ASSOCIATED CONTENT

### Ⓢ Supporting Information

NMR spectra of the organic compounds, HPLC traces of the oligonucleotides, UV, CD, and fluorescence data. This material is available free of charge via the Internet at http://pubs.acs.org.

## ■ AUTHOR INFORMATION


### Corresponding Author

*E-mail: robert.haener@dcb.unibe.ch.

### Present Address

Alina Nussbaumer, School of Chemistry, University of Manchester, Oxford Road, Manchester, M13 9PL, United Kingdom


### Notes

The authors declare no competing financial interest.

## ■ ACKNOWLEDGMENTS

We thank Dr. V. L. Malinovskii for helpful discussions. We thank Y. Vyborna for the preparation of the art work. Financial support by the Swiss National Foundation (grant 200020_149148) is gratefully acknowledged.

## ■ REFERENCES


(1) Panda, M. K., Ladomenou, K., and Coutsolelos, A. G. (2012) Porphyrins in bio-inspired transformations: light-harvesting to solar cell. *Coord. Chem. Rev. 256*, 2601−2627.

(2) Satake, A., and Kobuke, Y. (2007) Artificial photosynthetic systems: assemblies of slipped cofacial porphyrins and phthalocyanines showing strong electronic coupling. *Org. Biomol. Chem. 5*, 1679−1691.

(3) Drain, C. M. (2002) Self-organization of self-assembled photonic materials into functional devices: photo-switched conductors. *Proc. Natl. Acad. Sci. U. S. A 99*, 5178−5182.

(4) Babu, S. S., and Bonifazi, D. (2014) Self-organization of polar porphyrinoids. *ChemPlusChem 79*, 895−906.

(5) Nam, Y. S., Shin, T., Park, H., Magyar, A. P., Choi, K., Fantner, G., Nelson, K. A., and Belcher, A. M. (2010) Virus-templated assembly of porphyrins into light-harvesting nanoantennae. *J. Am. Chem. Soc. 132*, 1462−1463.

(6) Bahatyrova, S., Frese, R. N., Siebert, C. A., Olsen, J. D., Van Der Werf, K. O., Van Grondelle, R., Niederman, R., Bullough, P. A., Otto, C., and Hunter, C. N. (2004) The native architecture of a photosynthetic membrane. *Nature 430*, 1058−1062.

(7) Choi, M. S., Yamazaki, T., Yamazaki, I., and Aida, T. (2004) Bioinspired molecular design of light-harvesting multiporphyrin arrays. *Angew. Chem., Int. Ed. 43*, 150−158.

(8) Imahori, H., Mori, Y., and Matano, Y. (2003) Nanostructured artificial photosynthesis. *J. Photochem. Photobiol. C: Photochem. Rev. 4*, 51−83.

(9) Green, B. R., and Parson, W. W. (2003) *Light-Harvesting Antennas in Photosynthesis*, Kluwer Academic Publishers, Dordrecht.
(10) Malinovskii, V. L., Wenger, D., and Häner, R. (2010) Nucleic acid-guided assembly of aromatic chromophores. *Chem. Soc. Rev. 39*, 410−422.
(11) Albinsson, B., Hannestad, J. K., and Börjesson, K. (2012) Functionalized DNA nanostructures for light harvesting and charge separation. *Coord. Chem. Rev. 256*, 2399−2413.
(12) Stulz, E. (2012) DNA architectonics: towards the next generation of bio-inspired materials. *Chem.−Eur. J. 18*, 4456−4469.
(13) Endo, M., and Sugiyama, H. (2009) Chemical approaches to DNA nanotechnology. *ChemBioChem 10*, 2420−2443.
(14) Pan, K., Boulais, E., Yang, L., and Bathe, M. (2014) Structure-based model for light-harvesting properties of nucleic acid nanostructures. *Nucleic Acids Res. 42*, 2159−2170.
(15) Varghese, R., and Wagenknecht, H. A. (2009) DNA as a supramolecular framework for the helical arrangements of chromophores: towards photoactive DNA-based nanomaterials. *Chem. Commun.*, 2615−2624.
(16) Weisbrod, S. H., and Marx, A. (2008) Novel strategies for the site-specific covalent labelling of nucleic acids. *Chem. Commun.*, 5675−5685.
(17) Teo, Y. N., and Kool, E. T. (2012) DNA-multichromophore systems. *Chem. Rev. 112*, 4221−4245.
(18) Filichev, V. V., and Pedersen, E. B. (2009) DNA-conjugated organic chromophores in DNA stacking interactions, in *Wiley Encyclopedia of Chemical Biology* (Begley, T. P., Ed.) pp 493−524, Wiley, Hoboken.
(19) Ostergaard, M. E., and Hrdlicka, P. J. (2011) Pyrene-functionalized oligonucleotides and locked nucleic acids (LNAs): tools for fundamental research, diagnostics, and nanotechnology. *Chem. Soc. Rev. 40*, 5771−5788.
(20) Astakhova, I. K., and Wengel, J. (2014) Scaffolding along nucleic acid duplexes using 2′-amino-locked nucleic acids. *Acc. Chem. Res. 47*, 1768−1777.
(21) Nakamura, M., Shimomura, Y., Ohtoshi, Y., Sasa, K., Hayashi, H., Nakano, H., and Yamana, K. (2007) Pyrene aromatic arrays on RNA duplexes as helical templates. *Org. Biomol. Chem. 5*, 1945−1951.
(22) Yang, D. Y., Campolongo, M. J., Tran, T. N. N., Ruiz, R. C. H., Kahn, J. S., and Luo, D. (2010) Novel DNA materials and their applications. *WIREs Nanomed. Nanobiotech. 2*, 648−669.
(23) Aldaye, F. A., Palmer, A. L., and Sleiman, H. F. (2008) Assembling materials with DNA as the guide. *Science 321*, 1795−1799.
(24) Feldkamp, U., and Niemeyer, C. M. (2006) Rational design of DNA nanoarchitectures. *Angew. Chem., Int. Ed. 45*, 1856−1876.
(25) Goodchild, J. (1990) Conjugates of oligonucleotides and modified oligonucleotides: a review of their synthesis and properties. *Bioconjugate Chem. 1*, 165−187.
(26) Beaucage, S. L., and Iyer, R. (1993) The functionalization of oligonucleotides via phosphoramidite derivatives. *Tetrahedron 49*, 1925−1963.
(27) El-Sagheer, A. H., and Brown, T. (2010) Click chemistry With DNA. *Chem. Soc. Rev. 39*, 1388−1405.
(28) Cobb, A. J. A. (2007) Recent highlights in modified oligonucleotide chemistry. *Org. Biomol. Chem. 5*, 3260−3275.
(29) Berlin, K., Jain, R. K., Simon, M. D., and Richert, C. (1998) A porphyrin embedded in DNA. *J. Org. Chem. 63*, 1527−1535.
(30) Grabowska, I., Singleton, D. G., Stachyra, A., Gora-Sochacka, A., Sirko, A., Zagorski-Ostoja, W., Radecka, H., Stulz, E., and Radecki, J. (2014) A highly sensitive electrochemical genosensor based on co-porphyrin-labelled DNA. *Chem. Commun. 50*, 4196−4199.
(31) Choi, J. K., Sargsyan, G., Olive, A. M., and Balaz, M. (2013) Highly sensitive and selective spectroscopic detection of mercury(II) in water by using pyridylporphyrin-DNA conjugates. *Chem.—Eur. J. 19*, 2515−2522.
(32) Burns, J. R., Göpfrich, K., Wood, J. W., Thacker, V. V., Stulz, E., Keyser, U. F., and Howorka, S. (2013) Lipid-bilayer-spanning DNA nanopores with a bifunctional porphyrin anchor. *Angew. Chem., Int. Ed. 52*, 12069−12072.
(33) Woller, J. G., Hannestad, J. K., and Albinsson, B. (2013) Self-assembled nanoscale DNA−porphyrin complex for artificial light harvesting. *J. Am. Chem. Soc. 135*, 2759−2768.
(34) Borjesson, K., Wiberg, J., and El-Sagheer, A. H. (2010) Functionalized nanostructures: redox-active porphyrin anchors for supramolecular DNA assemblies. *ACS Nano 4*, 5037−5046.
(35) Nguyen, T., Brewer, A., and Stulz, E. (2009) Duplex stabilization and energy transfer in zipper porphyrin-DNA. *Angew. Chem., Int. Ed. 48*, 1974−1977.
(36) Endo, M., Seeman, N. C., and Majima, T. (2005) DNA tube structures controlled by a four-way-branched DNA connector. *Angew. Chem., Int. Ed. 44*, 6074−6077.
(37) Sargsyan, G., and Balaz, M. (2012) Porphyrin−DNA conjugates: porphyrin induced adenine−guanine homoduplex stabilization and interduplex assemblies. *Org. Biomol. Chem. 10*, 5533.
(38) Balaz, M., Holmes, A. E., Benedetti, M., Rodriguez, P. C., Berova, N., Nakanishi, K., and Proni, G. (2005) Synthesis and circular dichroism of tetraarylporphyrin-oligonucleotide conjugates. *J. Am. Chem. Soc. 127*, 4172−4173.
(39) Mammana, A., Pescitelli, G., Asakawa, T., Jockusch, S., Petrovic, A. G., Monaco, R. R., Purrello, R., Turro, N. J., Nakanishi, K., Ellestad, G. A., Balaz, M., and Berova, N. (2009) Environmental factors on the structure and spectroscopic response of 5′-DNA−porphyrin conjugates caused by changes in the porphyrin−porphyrin interactions. *Chem.−Eur. J. 15*, 11853−11866.
(40) Balaz, M., Bitsch-Jensen, K., Mammana, A., Ellestad, G. A., Nakanishi, K., and Berova, N. (2007) Porphyrins as spectroscopic sensors for conformational studies of DNA. *Pure Appl. Chem. 79*, 801−809.
(41) Balaz, M., Li, B. C., Jockusch, S., Ellestad, G. A., and Berova, N. (2006) Tetraarylporphyrin as a selective molecular cap for non-watson-crick guanine-adenine base-pair sequences. *Angew. Chem., Int. Ed. 45*, 3530−3533.
(42) Fendt, L. A., Bouamaied, I., Thoeni, S., Amiot, N., and Stulz, E. (2007) DNA as supramolecular scaffold for porphyrin arrays on the nanometer scale. *J. Am. Chem. Soc. 129*, 15319−15329.
(43) Casas, C., Lacey, C. J., and Meunier, B. (1993) Preparation of hybrid DNA cleaver oligonucleotide molecules based on a metallotris-(methylpyridiniumyl)porphyrin motif. *Bioconjugate Chem. 4*, 366−371.
(44) Le Doan, T., Praseuth, D., Perrouault, L., Chassignol, M., Thuong, N. T., and Helene, C. (1990) Sequence-targeted photochemical modifications of nucleic acids by complementary oligonucleotides covalently linked to porphyrins. *Bioconjugate Chem. 1*, 108−113.
(45) Fedorova, O. S., Savitskii, A. P., Shoikhet, K. G., and Ponomarev, G. V. (1990) Palladium(II)-coproporphyrin-I as a photoactivable group in sequence-specific modification of nucleic-acids by oligonucleotide derivatives. *FEBS Lett. 259*, 335−337.
(46) Mastruzzo, L., Woisard, A., Ma, D. D. F., Rizzarelli, E., Favre, A., and Le Doan, T. (1994) Targeted photochemical modification of HIV-derived oligoribonucleotides by antisense oligodeoxynucleotides linked to porphyrins. *Photochem. Photobiol. 60*, 316−322.
(47) Mestre, B., Jakobs, A., Pratviel, G., and Meunier, B. (1996) Structure/nuclease activity relationships of DNA cleavers based on cationic metalloporphyrin-oligonucleotide conjugates. *Biochemistry 2960*, 9140−9149.
(48) Morales-Rojas, H., and Kool, E. T. (2002) A porphyrin C-nucleoside incorporated into DNA. *Org. Lett. 4*, 4377−4380.
(49) Endo, M., Shiroyama, T., Fujitsuka, M., and Majima, T. (2005) Four-way-branched DNA-porphyrin conjugates for construction of four double-helix-DNA assembled structures. *J. Org. Chem. 70*, 7468−7472.
(50) Murashima, T., Hayata, K., Saiki, Y., Matsui, J., Miyoshi, D., Yamada, T., Miyazawa, T., and Sugimoto, N. (2007) Synthesis, structure and thermal stability of fully hydrophobic porphyrin−DNA conjugates. *Tetrahedron Lett. 48*, 8514−8517.
(51) Brewer, A., Siligardi, G., Neylon, C., and Stulz, E. (2011) Introducing structural flexibility into porphyrin-DNA zipper arrays. *Org. Biomol. Chem. 9*, 777−782.

(52) Sitaula, S., and Reed, S. M. (2008) Porphyrin conjugated to DNA by a 2′-amido-2′s-deoxyuridine linkage. *Bioorg. Med. Chem. Lett. 18*, 850−855.
(53) Mammana, A., Asakawa, T., Bitsch-Jensen, K., Wolfe, A., Chaturantabut, S., Otani, Y., Li, X., Li, Z., Nakanishi, K., Balaz, M., Ellestad, G. A., and Berova, N. (2008) Synthesis and characterization of water-soluble free-base, zinc and copper porphyrin−oligonucleotide conjugates. *Bioorg. Med. Chem. 16*, 6544−6551.
(54) Stephenson, A. W. I., Partridge, A. C., and Filichev, V. V. (2011) Synthesis of B−pyrrolic-modified porphyrins and their incorporation into DNA. *Chem.−Eur. J. 17*, 6227−6238.
(55) Clavé, G., Chatelain, G., Filoramo, A., Gasparutto, D., Saint-Pierre, C., Le Cam, E., Piétrement, O., Guérineau, V., and Campidelli, S. (2014) Synthesis of a multibranched porphyrin-oligonucleotide scaffold for the construction of DNA-based nano-architectures. *Org. Biomol. Chem. 12*, 2778−2783.
(56) Wellner, C., and Wagenknecht, H. A. (2014) Synthesis of DNA conjugates with metalated tetracationic porphyrins by postsynthetic cycloadditions. *Org. Lett. 16*, 1692−1695.
(57) Ohya, Y., Hashimoto, N., Jo, S., Nohori, T., Yoshikuni, T., Ouchi, T., and Tamiaki, H. (2009) Synthesis of oligo-DNA containing hydrophilic porphyrin in the main chain, and its energy transfer behaviour in duplex state. *Supramol. Chem. 21*, 301−309.
(58) Zhou, H., Johnson, A. T., Wiest, O., and Zhang, L. L. (2011) Incorporation of porphyrin acetylides into duplexes of the simplified nucleic acid GNA. *Org. Biomol. Chem. 9*, 2840−2849.
(59) Laha, J. K., Dhanalekshmi, S., Taniguchi, M., Ambroise, A., Lindsey, J. S., Carolina, N., and Uni, S. (2003) A scalable synthesis of meso-substituted dipyrromethanes. *Org. Process Res. Dev. 7*, 799−812.
(60) Asanuma, H., Fujii, T., Kato, T., and Kashida, H. (2012) Coherent interactions of dyes assembled on DNA. *J. Photochem. Photobiol., C 13*, 124−135.
(61) Hunter, C. A., Sanders, J. K. M., and Stone, A. J. (1989) Exciton coupling in porphyrin dimers. *Chem. Phys. 133*, 395−404.
(62) Stephenson, A. W. I., Bomholt, N., Partridge, A. C., and Filichev, V. V. (2010) Significantly enhanced DNA thermal stability resulting from porphyrin H-aggregate formation in the minor groove of the duplex. *Chembiochem 11*, 1833−1839.
(63) Endo, M., Fujitsuka, M., and Majima, T. (2008) Diastereochemically controlled porphyrin dimer formation on a DNA duplex scaffold. *J. Org. Chem. 73*, 1106−1112.
(64) Maiti, N. C., Ravikanth, M., Mazumdar, S., and Periasamy, N. (1995) Fluorescence dynamics of noncovalently linked porphyrin dimers and aggregates. *J. Phys. Chem. 99*, 17192−17197.
(65) See e.g. Rösch, U., Yao, S., Wortmann, R., and Würthner, F. (2006) Fluorescent H-aggregates of merocyanine dyes. *Angew. Chem., Int. Ed. 45*, 7026−7030 and references cited therein..
(66) Huang, X., Nakanishi, K., and Berova, N. (2000) Porphyrins and metalloporphyrins: versatile circular dichroic reporter groups for structural studies. *Chirality 255*, 237−255.
(67) Matile, S., Berova, N., and Nakanishi, K. (1995) Porphyrins: powerful chromophores for structural studies by exciton-coupled circular dichroism. *J. Am. Chem. Soc. 117*, 7021−7022.
(68) Balaz, M., Steinkruger, J. D., Ellestad, G. A., and Berova, N. (2005) 5 ′-Porphyrin-oligonucleotide conjugates: neutral porphyrin-DNA interactions. *Org. Lett. 7*, 5613−5616.
(69) Pasternack, R. F., Gibbs, E. J., and Villafranca, J. J. (1983) Interactions of porphyrins with nucleic-acids. *Biochemistry 22*, 2406−2414.
(70) Malinovskii, V. L., Nussbaumer, A. L., and Häner, R. (2012) Oligopyrenotides: chiral nanoscale templates for chromophore assembly. *Angew. Chem., Int. Ed. 51*, 4905−4908.
(71) Gibbs, E. J., Tinoco, I., Maestre, M. F., Ellinas, P. A., and Pasternack, R. F. (1988) Self-assembly of porphyrins on nucleic-acid templates. *Biochem. Biophys. Res. Commun. 157*, 350−358.
(72) Pescitelli, G., Gabriel, S., Wang, Y., Fleischhauer, J., Woody, R. W., and Berova, N. (2003) Theoretical analysis of the porphyrin-porphyrin exciton interaction in circular dichroism spectra of dimeric tetraarylporphyrins. *J. Am. Chem. Soc. 125*, 7613−7628.